Journal of Non-Crystalline Solids 375 (2013) 83–87

Contents lists available at SciVerse ScienceDirect

Journal of Non-Crystalline Solids

journal homepage: www.elsevier.com/ locate/ jnoncrysol

Achieving superior glass forming ability of Zr–Cu–Al–Ni–Ti/Ag bulk metallic glasses by element substitution

Xiao Cui, Fang-qiu Zu *, Wei-xin Jiang, Li-fang Wang, Zhi-zhi Wang

Institute of Liquid/Solid Metal Processing, School of Materials Science Engineering, Hefei University of Technology, Hefei 230009, People's Republic of China

ARTICLE INFO

Article history:
Received 19 February 2013
Received in revised form 9 May 2013
Available online 10 June 2013

Keywords:
Bulk metallic glass;
Glass forming ability;
Atomic packing fraction;
Mechanical property

ABSTRACT

In the present paper, glass forming ability (GFA) of $Zr_{57}Cu_{20}Al_{10}Ni_8Ti_{5-x}Ag_x$ ($x = \mathbf{0}$, 1, 2, 3, 4, 5) bulk metallic glasses (BMGs) are studied using conventional copper mold suction casting method. The critical diameter of amorphous rod is improved from 8 mm of $Zr_{57}Cu_{20}Al_{10}Ni_8Ti_5$ to 20 mm of $Zr_{57}Cu_{20}Al_{10}Ni_8Ag_5$ by fully substituting Ti with Ag. The great improvement of GFA is attributed to the enlarged negative mixing enthalpy, large atomic packing fraction, and low critical cooling rate, which are −32.026 kJ/mol, 0.761, and 2.5 K/s, respectively. The mechanical property is also improved by substituting Ti with Ag. The yield strength, ultimate strength and plastic strain are enhanced from (1469 MPa, 1490 MPa and 0.1%) for $Zr_{57}Cu_{20}Al_{10}Ni_8Ti_5$ BMG to (1612 MPa, 1746 MPa and 2.1%) for $Zr_{57}Cu_{20}Al_{10}Ni_8Ag_5$ BMG, respectively.

1. Introduction

Zr-based BMGs have shown a combination of unique properties such as high GFA [1,2], high strength [3], high plasticity [4], high corrosion resistance [5] etc. Up to date, Zr-based BMGs have been developed in various alloy systems including Zr–Al–Ni–Cu, Zr–Cu–Ag–Al, Zr–Ti–Cu–Ni–Be, Zr–Cu–Al–Ni–Ti and Zr–Cu–Ag–Al–Be [1–8]. Inoue [9] had proposed three empirical rules on formation of BMGs, which include: (1) multi-component alloys of three or more elements; (2) more than 12% atomic radius atomic mismatch between the main components; (3) large negative heat of mixing between the main elements. The atomic configuration of these complicated structures usually corresponds to higher degree of the dense random packed structures which lead to high viscous of the super-cooled liquid states and slow crystallization [9,10]. The effects of multi-component and large atomic mismatch are summarized as "confuse principle" [11].

Various glass forming systems will give us more choice for selecting BMGs with unique properties, and improving the GFA and mechanical property is significant in the development of BMGs for possible application as engineering materials. There are numerous approaches to improve the GFA of BMGs, such as minor element addition [12–14], element substitution [15,16] and controlling the melt temperature [17] etc. The minor addition or element substitution, i.e., the intentional introduction of impurities into a material, is fundamental to controlling the formation, manufacture, and properties of various materials [13]. In the present research, by substituting Ti with Ag, the critical diameter of metallic glass rod is improved from 8 mm of the initial alloy $Zr_{57}Cu_{20}Al_{10}Ni_8Ti_5$ to 20 mm of $Zr_{57}Cu_{20}Al_{10}Ni_8Ag_5$ alloy. The GFA is discussed in terms of size effect, mixing enthalpy, packing fraction, and critical cooling rate. The results indicate that the increase of packing fraction and mixing enthalpy should be the reason for the improvement of GFA.

2. Experimental

Multi-component alloy ingots with nominal compositions of $Zr_{57}Cu_{20}Al_{10}Ni_8Ti_{5-x}Ag_x$ ($x = 0$, 1, 2, 3, 4, 5) were prepared by arc melting mixtures of elements with purity higher than 99.9 at.% in high purity argon atmosphere. Each ingot was melted five times in the arc melter accompanied with electromagnetic stirring to ensure the chemical homogeneity. Ingots were remelted and sucked into water cooled copper molds, and the copper molds have internal cylindrical cavities with diameters of 5 mm (Φ5), 8 mm (Φ8), 10 mm (Φ10), 12 mm (Φ12), 14 mm (Φ14), and 20 mm (Φ20). The structure of the as cast rods was examined by D/MAX-2500V X-ray diffractometer with Cu-Kα radiation (XRD) and JOEL JEM-2100F high resolution transmission electron microscope (HRTEM). GFA associated with glass transition and thermal stability was examined using Perkin-Elmer DSC-8000 differential scanning calorimetry (DSC) with a heating rate of 40 K/min. The pieces that used for both XRD and DSC analyses were cut from the top of the samples. The melt temperature and liquid temperature were examined on Perkin-Elmer DTA-7 at a heating rate of 10 K/min.

The density of these samples was measured by Archimedes method, using a density balance named Shimadzu GH-124S with the accuracy of 10^{-4} g (by measuring the mass of the sample in air (m_a) and in pure water (m_w) respectively, concerning the density of water (ρ_w) with corresponding temperature, the density of the sample can be expressed as: $\rho = (m_a\rho_w)/(m_a - m_w)$). Mechanical properties were measured at room temperature with an MTS 809 system at a strain rate of 10^{-4} s^{-1}.

* Corresponding author. Tel./fax: +86 551 62905057.
E-mail address: fangqiuzu@hotmail.com (F. Zu).

0022-3093/$ – see front matter © 2013 Elsevier B.V. All rights reserved.
http://dx.doi.org/10.1016/j.jnoncrysol.2013.05.014

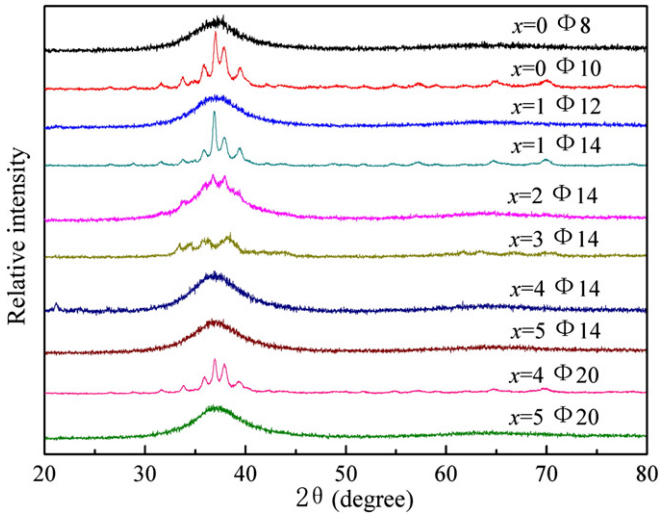

Fig. 1. XRD patterns of as cast $Zr_{57}Cu_{20}Al_{10}Ni_8Ti_{5-x}Ag_x$ ($x = 0, 1, 2, 3, 4, 5$) BMGs related with their critical diameter.

The dimension of the samples used for compression test is $\Phi 5 \times 10$ mm. The fracture surface of the BMGs was investigated by a JSM-6490LV scanning electron microscopy (SEM).

3. Results and discussion

$Zr_{57}Cu_{20}Al_{10}Ni_8Ti_5$ BMG was first reported by Xing et al. [5], and rod of $\Phi 10$ with fully amorphous state can be cast. However, in our previous work [18], only $\Phi 8$ rod can be cast, by substituting 1 at.% Ti with Ag, $\Phi 12$ rod with fully amorphous structure can be cast. This work gives further information on GFA by substituting more Ti with Ag, and the results are shown in Fig. 1. As shown in Fig. 1, for the samples of the rod $\Phi 10$ of $x = 0$, $\Phi 14$ of $x = 1$, $\Phi 14$ of $x = 2$, $\Phi 14$ of $x = 3$, and $\Phi 20$ of $x = 4$, all the sharp Bragg peaks indicate that they are not fully amorphous. Contrarily, the typical broad diffraction maxima signify that the rod $\Phi 8$ of $x = 0$, $\Phi 12$ of $x = 1$, $\Phi 14$ of $x = 4$, $\Phi 14$ of $x = 5$, and $\Phi 20$ of $x = 5$ is fully amorphous structure.

Fig. 2(a) shows the as-cast sample of $Zr_{57}Cu_{20}Al_{10}Ni_8Ag_5$ BMG with 20 mm diameter and $Zr_{57}Cu_{20}Al_{10}Ni_8Ti_4Ag_1$ BMG with 14 mm diameter. The HRTEM image and selected-area electron diffraction shown in Fig. 2(b) further confirm the structure of the cross section of the as cast $\Phi 20$ $Zr_{57}Cu_{20}Al_{10}Ni_8Ag_5$ BMG is amorphous. It should be noted that the positive heat of mixing between Cu–Ag may introduce phase separation, and in the work of Fujita et al. [19], they found that for $Cu_{50}Zr_{50}$ BMG, adding 10% Ag could obviously improve the GFA; however, adding 20% Ag induced phase separation. According to the HRTEM imagine in this work, adding Ag to $Zr_{57}Cu_{20}Al_{10}Ni_8Ti_5$ BMG does not induce phase separation for all the samples. The results indicate that with more Ag substituting Ti in $Zr_{57}Cu_{20}Al_{10}Ni_8Ti_5$ alloy, more greatly the GFA could be improved, $\Phi 20$ rod with fully amorphous structure can be cast for the alloy $Zr_{57}Cu_{20}Al_{10}Ni_8Ag_5$.

Fig. 3 shows the DSC traces of the as cast $Zr_{57}Cu_{20}Al_{10}Ni_8Ti_{5-x}Ag_x$ ($x = 0, 1, 2, 3, 4, 5$) BMGs. All the traces show apparent endothermic phenomenon caused by glass transition and exothermic phenomenon caused by crystallization. The characteristic parameters are shown in Table 1. The results show that the glass transition temperature (T_g) has no significant change with the increase of Ag content. Nevertheless, the crystallization temperature (T_x) increases significantly with the increase of Ag content. The $Zr_{57}Cu_{20}Al_{10}Ni_8Ag_5$ BMG has the highest crystallization temperature, which is 779.3 K, and correspondingly, the supercooled liquid region [20] ($\Delta T_x = T_x - T_g$), reduced glass transition temperature [21] ($T_{rg} = T_g/T_m$) and parameter γ [22] ($T_x/(T_g + T_l)$) are 110.9 K, 0.603, and 0.433, respectively. The results indicate that the $Zr_{57}Cu_{20}Al_{10}Ni_8Ag_5$ BMG has super-high GFA, and the large ΔT_x and T_x values indicate that the supercooled liquid of the $Zr_{57}Cu_{20}Al_{10}Ni_8Ag_5$ BMG also has super-high thermal-stability against crystallization.

The critical cooling rate which required a metallic glass to avoid the formation of detectable fraction of crystal in quenching molten alloys is used to describe the glass forming ability of materials. The maximum D_c (take the centimeter sized data) for which samples is fully amorphous structures can be used to estimate the critical cooling rate R_c, according to the following formula [23]:

$$R_c(K/s) = 10/[D_c(cm)]^2. \quad (1)$$

As the maximum D_c for $Zr_{57}Cu_{20}Al_{10}Ni_8Ag_5$ BMG is 20 mm, using Eq. (1), the R_c for $Zr_{57}Cu_{20}Al_{10}Ni_8Ag_5$ BMG is estimated to be smaller than 2.5 K/s. The low critical cooling rate of $Zr_{57}Cu_{20}Al_{10}Ni_8Ag_5$ would facilitate the formation of amorphous structure with large size when quenching the melt into copper mold.

The ordinary guiding principles on designing multi-component BMGs [9] indicate that the atomic mismatch between elements should be more than 12% and the negative heat of mixing between the elements should be large. The dramatic difference in size and large negative heat of mixing would lead to strong atomic interactions and cause an increasing confusion of multi-component alloy system, and lead the elements attractively arranged to each other whenever possible,

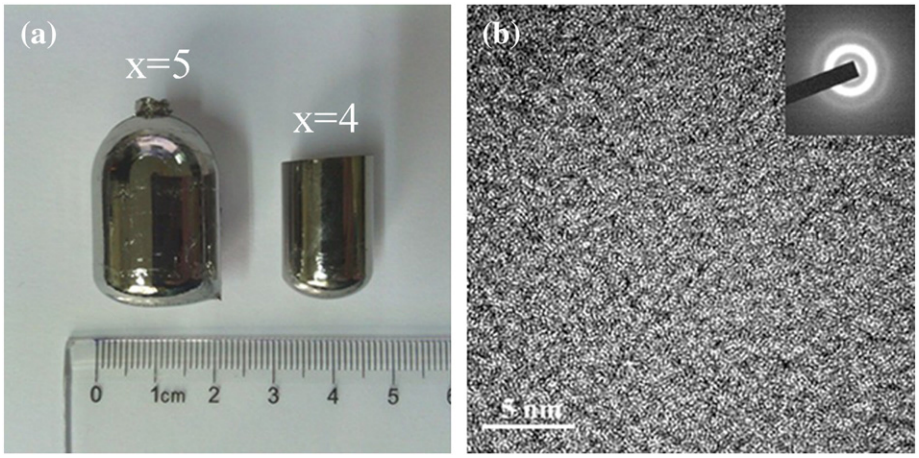

Fig. 2. (a) As-cast sample of $Zr_{57}Cu_{20}Al_{10}Ni_8Ag_5$ BMG with 20 mm diameter and $Zr_{57}Cu_{20}Al_{10}Ni_8Ti_4Ag_1$ BMG with 14 mm diameter. (b) An HRTEM micrograph of the cross section of the as cast 20 mm diameter $Zr_{57}Cu_{20}Al_{10}Ni_8Ag_5$ BMG; the inset shows the selected-area electron diffraction.

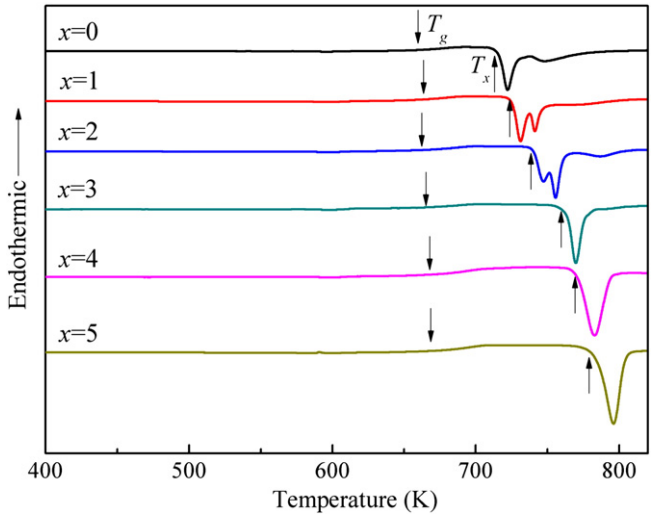

Fig. 3. DSC curves of as cast $Zr_{57}Cu_{20}Al_{10}Ni_8Ti_{5-x}Ag_x$ ($x = 0, 1, 2, 3, 4, 5$) BMGs with a heating rate of 40 K/min.

which would reduce the energetic advantage of forming an ordered structure of long range periodicity. The mixing enthalpy (ΔH^{mix}) of BMGs could be calculated by the equation [24]:

$$\Delta H^{mix} = \sum_{i \neq j} 4\Delta H_{ij}^{mix} x_i x_j. \quad (2)$$

The values of ΔH_{ij}^{mix} were obtained from literature [25] which are calculated by Miedema's model. x_i and x_j are the atomic percentage of the element i and j. The calculated mixing enthalpy is shown in Table 1, ΔH^{mix} decreases with Ag content increasing, and $Zr_{57}Cu_{20}Al_{10}Ni_8Ag_5$ BMG has the largest negative heat of mixing. It suggests that the improvement of the GFA by substituting Ti with Ag in this work is quite in agreement with Inoue's mixing enthalpy criteria.

The atomic mismatch criterion on designing multi-component BMGs means that the high GFA BMGs should have high atomic packing state. In order to get more detailed information on the atomic packing state, atomic packing fraction of as cast $Zr_{57}Cu_{20}Al_{10}Ni_8Ti_{5-x}Ag_x$ ($x = 0, 1, 2, 3, 4, 5$) BMGs was compared. The density (ρ) data of the BMGs were measured, and from which atomic packing fraction (K) was obtained to analyze the relation between GFA and atomic packing status. The packing fraction of BMGs could be approximately expressed as follows:

$$K = \frac{\sum n_i v_i}{V}. \quad (3)$$

where n_i and v_i ($v_i = 4/3\pi r_i^3$, the data of r_i were obtained from literature [26]) represents respectively the number of atoms and the atomic volume for each element in unit volume, the sum of $n_i v_i$ can express the volume of all the atoms. And V represents the unit volume (1 cm^3). The mass of the BMGs with unit volume could be calculated from the density data, and then n_i could be calculated.

The data of the measured density and the calculated atomic packing fraction as well as their variation tendency are shown in Table 1 and Fig. 4. It was reported [27–29] that the GFA is believed to be related with the degree of dense packing in metallic glasses, and the discovered BMGs are usually reported to have a high degree of dense packed atomic structures. As it can be seen in Fig. 4, the measured density has nearly direct proportion with the increase of Ag content. The density is increased from 6.516 g/cm^3 of $Zr_{57}Cu_{20}Al_{10}Ni_8Ti_5$ BMG to 6.926 g/cm^3 of $Zr_{57}Cu_{20}Al_{10}Ni_8Ag_5$ BMG by fully substituting Ti with Ag. Although the overall trend of the calculated packing fraction has direct proportion with the increase of Ag content, the packing fraction of the $x = 3$(0.752) and $x = 2$(0.752) BMGs is lower than that of $x = 1$ BMG (0.754). The density data can show the apparent atomic packing state of a BMG, while the atomic packing fraction will show us the intrinsic atomic packing state of BMGs. The changing trend in the density and the packing fraction with respect to the Ag content indicate that the GFA is correlated with the atomic packing state in $Zr_{57}Cu_{20}Al_{10}Ni_8Ti_{5-x}Ag_x$ ($x = 0, 1, 2, 3, 4, 5$) BMGs.

The highest atomic packing fraction of $Zr_{57}Cu_{20}Al_{10}Ni_8Ag_5$ BMG implies the highest packing density of the component atoms, which cause the arrangement of the atoms more closely. It was reported [30] that the higher packing density achieves the higher GFA through the decrease of atomic diffusivity and the increase of viscosity. In the higher degree of atomic packing state, the atomic rearrangements of the constituent elements are suppressed, leading to the decrease of atomic mobility and the increase of viscosity. Furthermore, the frequency at which the atoms are attached at the liquid/solid interface decreases in the higher degree of dense random packed structure, leading to the decrease of the nucleation frequency of a crystalline phase [30]. Therefore, a higher degree of dense random packing would strongly hinder the formation of orderly arrayed crystal structures when quenching the alloy melt into copper mold, and the higher packing fraction is believed to be an important influencing factor in improving the GFA of BMGs.

As new glass forming compositions with high GFA and potential engineering applications, it is important to test the mechanical properties of the as cast BMGs. Fig. 5(a) shows the compressive stress–strain curves of $Zr_{57}Cu_{20}Al_{10}Ni_8Ti_{5-x}Ag_x$ ($x = 0, 1, 2, 3, 4, 5$) BMGs. The yield strength σ_y, ultimate compression stress σ_{max}, and plastic strain ε_p of the samples are summarized in Table 2. It can be seen that the Ag free alloy ($x = 0$) exhibits a yield strength of ~1469 MPa, an ultimate strength of ~1490 MPa, and nearly no plastic strain. However, for the best glass former, $Zr_{57}Cu_{20}Al_{10}Ni_8Ag_5$, it exhibits the yield strength of ~1612 MPa, an ultimate strength of ~1746 MPa, and a plastic strain of ~2.11%.

The morphology of the fracture surface is shown in Fig. 5(b–c), the compressive shear fracture angle is measured to be ~41.6°, which was considered to be a typical value of the initial shear angle of the primary shear band in such material [31,32]. The shear bands interaction and vein-like patterns as well as some melt drops shown in Fig. 5(c–d) reveal the apparent fracture characteristic of BMGs [14,15,33]. Compared with the original alloy composition ($Zr_{57}Cu_{20}Al_{10}Ni_8Ti_5$) the GFA and compressive strength of the new BMG ($Zr_{57}Cu_{20}Al_{10}Ni_8Ag_5$) are improved greatly. By fully replacing Ti with Ag, both the atomic packing fraction and the negative mixing enthalpy increased. So, substituting

Table 1
Thermal data, mixing enthalpy data, density data, and packing fraction data of as cast $Zr_{57}Cu_{20}Al_{10}Ni_8Ti_{5-x}Ag_x$ ($x = 0, 1, 2, 3, 4, 5$) BMGs.

Ag content (at.%)	T_g (K)	T_x (K)	ΔT_x (K)	T_m (K)	T_l (K)	Trg	γ	ΔH^{mix} (kJ/mol)	ρ (g/cm^3)	K
$x = 0$	660.6	715.2	54.6	1118.2	1153.7	0.591	0.394	−31.502	6.516	0.747
$x = 1$	663.2	725.9	62.7	1115.5	1149.3	0.595	0.400	−31.628	6.637	0.754
$x = 2$	662.3	738.4	76.1	1089.9	1153.5	0.607	0.406	−31.718	6.672	0.752
$x = 3$	663.5	759.7	96.2	1096.4	1124.4	0.605	0.424	−31.822	6.728	0.752
$x = 4$	668.4	769.2	100.8	1106.6	1127.1	0.604	0.423	−31.925	6.821	0.756
$x = 5$	668.4	779.3	110.9	1108.8	1135.1	0.603	0.433	−32.026	6.926	0.761

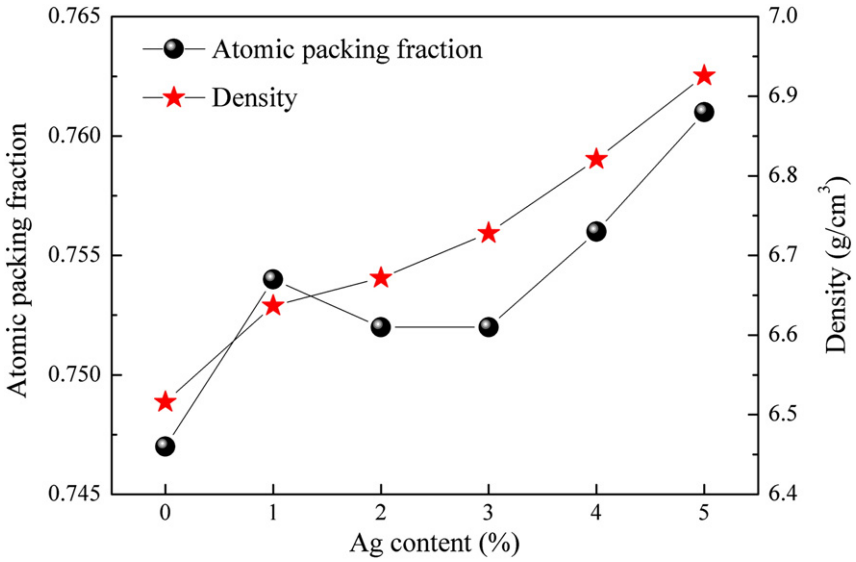

Fig. 4. Variation tendency of atomic packing fraction and density of as cast $Zr_{57}Cu_{20}Al_{10}Ni_8Ti_{5-x}Ag_x$ ($x = 0, 1, 2, 3, 4, 5$) BMGs with respect to Ag content.

Ti with Ag would promote the formation of short-range or medium-range ordered clusters, and the chemical inhomogeneity, which would benefit the activation of multiple shear bands and the improvement of ductility and strength of BMGs [14]. Although a significant plasticity of $Zr_{57}Cu_{20}Al_{10}Ni_8Ag_5$ BMG is not achieved, we believe that by further adjusting the atomic percentage of $Zr_{57}Cu_{20}Al_{10}Ni_8Ag_5$ BMG, new BMGs with pronounced mechanical property and GFA will be achieved.

4. Conclusion

The GFA improves with the increasing of Ag content in $Zr_{57}Cu_{20}Al_{10}Ni_8Ti_{5-x}Ag_x$ ($x = 0, 1, 2, 3, 4, 5$) BMGs system. The new alloy, $Zr_{57}Cu_{20}Al_{10}Ni_8Ag_5$, which has a critical cooling rate of only 2.5 K/s can easily be cast into fully glass rod with a diameter of 20 mm. The superior GFA is attributed to large negative mixing enthalpy of the alloy system and

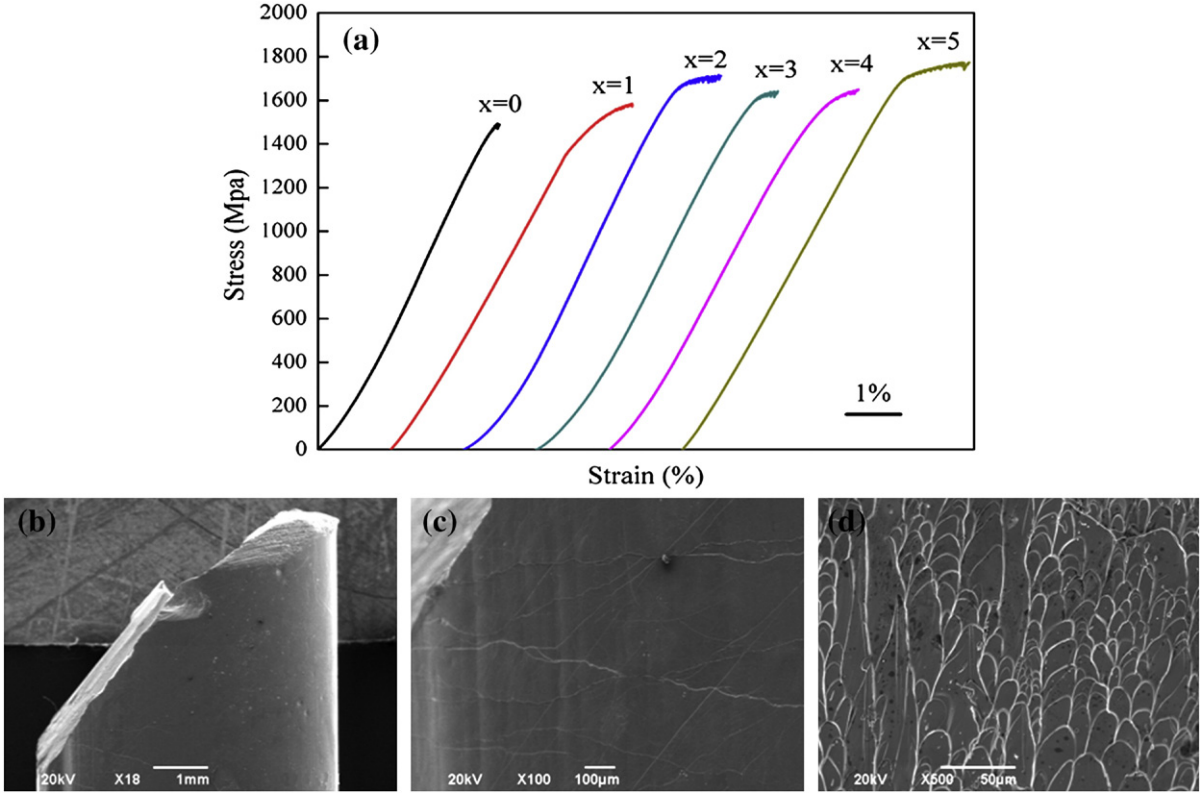

Fig. 5. (a) Compressive stress–strain curves at room temperature for $Zr_{57}Cu_{20}Al_{10}Ni_8Ti_{5-x}Ag_x$ ($x = 0, 1, 2, 3, 4, 5$) BMGs. (b)–(c) Side-view scanning electron micrographs of the fractured $Zr_{57}Cu_{20}Al_{10}Ni_8Ag_5$ sample. (d) Fracture surface of the fractured $Zr_{57}Cu_{20}Al_{10}Ni_8Ag_5$ sample.

Table 2
Compressive mechanical properties of $Zr_{57}Cu_{20}Al_{10}Ni_8Ti_{5-x}Ag_x$ ($x = 0, 1, 2, 3, 4, 5$) BMGs.

Ag content (at.%)	σ_y (Mpa)	σ_{max} (Mpa)	ε_p (%)	E (GPa)
$x = 0$	1469	1490	0.11	257.5
$x = 1$	1366	1582	0.87	279.2
$x = 2$	1579	1709	0.75	242.9
$x = 3$	1511	1636	0.52	218.9
$x = 4$	1481	1647	0.69	270.7
$x = 5$	1612	1746	2.11	284.3

the high atomic packing fraction. With the increasing of Ag content, the atomic packing fraction shifts from 0.747 of $-Ti_5Ag_0$ BMG to 0.761 of $-Ti_0Ag_5$ BMG. By fully substituting Ti with Ag, the yield strength, ultimate strength and plastic strain are enhanced from (1469 MPa, 1490 MPa and 0.1%) for $Zr_{57}Cu_{20}Al_{10}Ni_8Ti_5$ BMG to (1612 MPa, 1746 MPa and 2.1%) for $Zr_{57}Cu_{20}Al_{10}Ni_8Ag_5$ BMG, respectively. Experimental results in the present work indicate that by further adjusting the atomic percentage of $Zr_{57}Cu_{20}Al_{10}Ni_8Ag_5$ BMG, new BMGs with pronounced mechanical property and GFA could be achieved.

Acknowledgement

The authors are grateful for the financial support of the National Natural Science Foundation of China (Grant No. 50971053) and the National Basic Research Program of China (Grant No. 2012CB825702).

References

[1] A. Peker, W.L. Johnson, Appl. Phys. Lett. 63 (1993) 2342–2344.
[2] H.B. Lou, X.D. Wang, F. Xu, S.Q. Ding, Q.P. Cao, K. Hono, J.Z. Jiang, Appl. Phys. Lett. 99 (2011) 051910.
[3] A.S. Bakai, A.P. Shpak, N. Wanderka, S. Kotrechko, T.I. Mazilova, I.M. Mikhailovski, J. Non-Cryst. Solids 356 (2010) 1310–1314.
[4] Y.H. Liu, G. Wang, R.J. Wang, D.Q. Zhao, M.X. Pan, W.H. Wang, Science 315 (2007) 1385–1388.
[5] N.B. Hua, L. Huang, J.F. Wang, Y. Cao, S.J. Pang, T. Zhang, J. Non-Cryst. Solids 358 (2012) 1599–1604.
[6] L.Q. Xing, P. Ochin, M. Harmelin, F. Faudot, J. Bigot, J.P. Chevalier, Mater. Sci. Eng., A 220 (1996) 155–161.
[7] A. Inoue, T. Zhang, N. Nishiyama, K. Ohba, T. Masumoto, Mater. Trans. JIM 34 (1993) 1234–1237.
[8] A. Inoue, T. Zhang, Mater. Trans. JIM 37 (1996) 185–187.
[9] A. Inoue, Acta Mater. 48 (2000) 279–306.
[10] M.B. Tang, D.Q. Zhao, M.X. Pan, W.H. Wang, Chin. Phys. Lett. 21 (2004) 901–903.
[11] A.L. Greer, Nature 366 (1993) 303–304.
[12] X.L. Zhang, G. Chen, J. Non-Cryst. Solids 358 (2012) 1319–1323.
[13] W.H. Wang, Prog. Mater. Sci. 52 (2007) 540–596.
[14] P. Gong, K.F. Yao, Y. Shao, J. Alloys Compd. 536 (2012) 26–29.
[15] N. Khademian, R. Gholamipour, F. Shahri, M. Tamizifar, J. Alloys Compd. 546 (2013) 41–47.
[16] L.L. Zhang, R. Li, J.F. Wang, H.Y. Zhang, N.B. Hua, T. Zhang, J. Non-Cryst. Solids 358 (2012) 1425–1429.
[17] G. Kumar, T. Ohkubo, K. Hono, J. Mater. Res. 24 (2009) 2353–2360.
[18] X. Cui, B.C. Xu, Z.Z. Wang, L.F. Wang, B. Zhang, F.Q. Zu, Acta Phys. Sin. 62 (2013) 016101.
[19] T. Fujita, K. Konno, W. Zhang, V. Kumar, M. Matsuura, A. Inoue, T. Sakurai, M.W. Chen, Phys. Rev. Lett. 103 (2009) 075502.
[20] A. Inoue, T. Zhang, T. Masumoto, J. Non-Cryst. Solids 156–158 (1993) 473–480.
[21] D. Turnbull, Contemp. Phys. 10 (1969) 473–488.
[22] Z.P. Lu, C.T. Liu, Acta Mater. 50 (2002) 3501–3512.
[23] W.H. Wang, J.J. Lewandowski, A.L. Greer, J. Mater. Res. 20 (2005) 2307–2313.
[24] A.L. Zhang, D. Chen, Z.H. Chen, Intermetallics 18 (2010) 74–76.
[25] A. Takeuchi, A. Inoue, Mater. Trans. JIM 46 (2005) 2817–2829.
[26] O.N. Senkov, D.B. Miracle, Mater. Res. Bull. 36 (2001) 2183–2198.
[27] B.C. Xu, R.J. Xue, B. Zhang, Intermetallics 32 (2013) 1–5.
[28] A.L. Greer, Science 267 (1995) 1947–1953.
[29] Y.Q. Chen, E. Ma, Prog. Mater. Sci. 56 (2011) 379–473.
[30] A. Inoue, T. Negishi, H.M. Kimura, T. Zhang, A.R. Yavari, Mater. Trans. JIM 39 (1998) 318–321.
[31] D.D. Qu, K.D. Liss, Y.J. Sun, M. Reid, J.D. Almer, K. Yan, Y.B. Wang, X.Z. Liao, J. Shen, Acta Mater. 61 (2013) 321–330.
[32] Z.F. Zhang, G. He, H. Zhang, J. Eckert, Scr. Mater. 52 (2005) 945–949.
[33] W. Zhou, X. Lin, J.F. Li, J. Alloys Compd. 552 (2013) 102–106.